

AD-A198 887

DTIC FILE COPY

3

AFGL-TR-88-0178

RECENT ASTRONOMICAL RESULTS OBTAINED WITH THE AFGL TEN MICRON ARRAY SPECTROMETER

Paul D. LeVan and Peter C. Tandy
Air Force Geophysics Laboratory
Hanscom AFB, MA 01731-5000 USA

DTIC
ELECTE
SEP 01 1988
S H D

Abstract. The detector array used in the AFGL Spectrometer is the SBRC 58x62 Si:Ga with the switched-MOSFET readout (DRO). Support electronics include the clocked address circuitry, 12 bit AD conversion boards for each of the two output lines, and 20 bit RAM coaddition blocks for both telescope chop positions. In operation, the data are coadded over several chops, differences are taken between the two chop positions, and these differences are subsequently output to a PDP 11/34 minicomputer. The mosaic array was characterized for high speed operation (5 msec frame periodicity) and linearity in a test bed dewar, and found for proper bias voltages to be sufficiently fast to permit the signal electron rate from sky and telescope backgrounds. The optics are a NaCl prism slit spectrometer for operation in the 8 to 14 micron region. The ratio of collimator and camera focal lengths is 3.6, resulting in arcsec pixel sizes for the Wyoming Infrared Observatory (WIRO) 2.3 meter telescope. We report here on the recent observing run at WIRO, the second for the Array Spectrometer. The latest observing run resulted successfully in measurements of IRC + 10216 with the mosaic array in full scanning operation. Results include spectral and spatial scans for IRC + 10216 and evaluations of instrumental performance.

I. INTRODUCTION

The recent availability of large format infrared mosaic arrays for the ten micron region offers opportunities for both astronomical measurements from space as well as from groundbased telescopes. The two are complementary - the backgrounds in space are lower, the optics are smaller, and the observing time more restricted. For the case of groundbased telescopes, the optics can be quite large, but the background radiation levels from both the atmosphere and the telescope are extreme.

In this report we describe the Array Spectrometer electronics and optics, the testing of the array in the laboratory, and the results of using the spectrometer on the University of Wyoming 92" Telescope. The conclusions drawn relate to the appropriateness of the array architecture

The U.S. Government is authorized to reproduce and sell this report.
Permission for further reproduction by others must be obtained from
the copyright owner.

DISTRIBUTION STATEMENT A

Approved for public release
Distribution Unlimited

88 9 1 045

and material for use under these conditions, and the attractiveness of a continuing program of measurements of sources of infrared celestial radiation.

II. MOSAIC ARRAY AND SUPPORT ELECTRONICS

The detector arrangement in the AFGL spectrometer consists of a 58x62 Si:Ga MOSFET - switched array, which was lent to AFGL by Santa Barbara Research Center. The pixel spacing is 75 microns, for a total array size of 4.35x4.65mm. The quantum efficiency is claimed to be 40%, and the pixel well depth for linear operation is 3×10^6 electrons. Each array address (1798 total) corresponds to a pair of adjacent pixels, designated odd and even, with separate (odd and even) output lines. The on-chip amplification circuitry includes a first stage totum pole follower circuit for all charge integration sites, which are multi-plexed to a single second stage source follower for each of the two outputs. The output source follower resistance is off-chip and therefore selectable, and the values corresponding to low and high background operation are likely to be different, as noted below.

The analog signal processing chain consists of a gain 2 non-inverting operational amplifier selected for high slew rate and short settle time. The output of this amplifier charges a low-leakage storage capacitor which is resettable with a similarly low-leakage MOSFET switch, for clamping of the signal immediately prior to resetting the pixel charge storage site (White et al. 1973) Thus, the signal into the next (MOSFET-input) amplification stage is a running value with subtraction of the prior "signal plus reset level". The signal is sampled and converted to 12 bit resolution using Datel Model 868 convertors.

The requirements for the digital electronics design were driven at one extreme by the rapid "fill time" of typically 5 to 10 msec of the pixel charge storage sites under the expected background radiation levels. This data rate was sufficiently high as to require decimation in the form of RAM coadding rather than direct transfer to the mini-computer. An alternative to frame coaddition into RAM using arithmetic logic units is coaddition using microprocessors and programming instructions. Initially, advanced microprocessors (e.g., the Motorola 68020) were investigated but found not quite fast enough for the "worst case" data rate of 12 bit data words each microsecond.

Support electronics are divided into the array address generating board, the 12 bit analog to digital conversion boards (odd and even), the 20 bit RAM coaddition boards (odd and even), and the commercial timing pulse generators (one master, four slaves). All but the ADC electronics are located in a rack and cable-connected to the dewar (in which the mosaic array is maintained at a temperature of 4K); the ADC boards are mounted directly to the dewar for the shortest possible analog conductors.

REPORT DOCUMENTATION PAGE

1a. REPORT SECURITY CLASSIFICATION UNCLASSIFIED		1b. RESTRICTIVE MARKINGS	
2a. SECURITY CLASSIFICATION AUTHORITY		3. DISTRIBUTION/AVAILABILITY OF REPORT Approved for public release; Distribution unlimited	
2b. DECLASSIFICATION/DOWNGRADING SCHEDULE		5. MONITORING ORGANIZATION REPORT NUMBER(S)	
4. PERFORMING ORGANIZATION REPORT NUMBER(S) AFGL-TR-88-0178		7a. NAME OF MONITORING ORGANIZATION	
6a. NAME OF PERFORMING ORGANIZATION Air Force Geophysics Laboratory	6b. OFFICE SYMBOL (If applicable) OPC	7b. ADDRESS (City, State and ZIP Code)	
6c. ADDRESS (City, State and ZIP Code) Hanscom AFB Massachusetts, 01731-5000		9. PROCUREMENT INSTRUMENT IDENTIFICATION NUMBER	
8a. NAME OF FUNDING/SPONSORING ORGANIZATION	8b. OFFICE SYMBOL (If applicable)	10. SOURCE OF FUNDING NOS.	
8c. ADDRESS (City, State and ZIP Code)		PROGRAM ELEMENT NO.	PROJECT NO.
11. TITLE (Include Security Classification) (If) Recent Astronomical Results obtained with the AFGL Ten Micron Array Spectrometer		TASK NO.	WORK UNIT NO.
12. PERSONAL AUTHOR(S) LeVAN, PAUL D. and TANDY, PETER C.		62101F	7670
13a. TYPE OF REPORT Reprint		06	12
13b. TIME COVERED FROM 84 OCT TO 87 SEP		14. DATE OF REPORT (Yr., Mo., Day) 1988 August 27	
15. PAGE COUNT 11		16. SUPPLEMENTARY NOTATION Appeared in <u>IR Astronomy with Arrays</u> , University of Hawaii Workshop Proceedings.	
17. COSATI CODES		18. SUBJECT TERMS (Continue on reverse if necessary and identify by block number)	
FIELD	GROUP	SUB. GR.	
03	01	Infrared	
03	02	Celestial Sources	
19. ABSTRACT (Continue on reverse if necessary and identify by block number)		Spectroscopy	
The detector array used in the AFGL Spectrometer is the SBRC 58x62 Si:Ga with the switched-MOSFET readout (DRO). Support electronics include the clocked address circuitry, 12 bit AD conversion boards for each of the two output lines, and 20 bit RAM coaddition blocks for both telescope chop positions. The optics are a NaCl prism slit spectrometer for operation in the 8 to 14 micron region. The ratio of collimator and camera focal lengths is 3.6, resulting in arcsec pixel sizes for the Wyoming Infrared Observatory (WIRO) 2.3 meter telescope. We report here on the recent observing run at WIRO, the second for the ARRAY Spectrometer.			
20. DISTRIBUTION/AVAILABILITY OF ABSTRACT UNCLASSIFIED/UNLIMITED <input checked="" type="checkbox"/> SAME AS RPT. <input type="checkbox"/> DTIC USERS <input type="checkbox"/>		21. ABSTRACT SECURITY CLASSIFICATION UNCLASSIFIED	
22a. NAME OF RESPONSIBLE INDIVIDUAL PAUL D. LeVAN		22b. TELEPHONE NUMBER (Include Area Code) (617)377-4550	22c. OFFICE SYMBOL AFGL/OPC

The data collection scheme allows for coaddition of frames of data into blocks of RAM corresponding to the two telescope chop positions. Frame coaddition is suppressed over a selectable delay after chop transitions in order to allow for the chopping mirror settle time. Because the telescope secondary mirror chopping and array scanning must be synchronous, chopper TTL pulse frequency is generated which is selectable between 3 and 5 Hz. After several chops (typically 3 to 7), the data for the two chop positions are differenced and output on a pixel by pixel basis over a 16 bit bus to a field-transportable PDP 11/34, in typically 100 msec per frame. The cycle repeats as required by the operator.

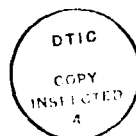
III. SODIUM CHLORIDE PRISM SLIT SPECTROMETER

The choice of reimaging optics between the telescope focus and the detector array was based on constraints posed by ground based astronomical observations in the ten micron region, specifically the high background radiation levels from both the atmosphere and telescope, and on the desire to observe all wavelength resolution elements simultaneously across one axis of the mosaic array, to minimize the effects of variations in atmospheric transmission. The resulting Sodium Chloride prism design has the properties described in Table I.

TABLE I

Sodium Chloride Prism Slit Spectrometer

Collimator mirror focal length	270 mm
Camera mirror focal length	75 mm
Collimated beam diameter	1 cm
Prism Angles: apex/incidence/deviation	55°/48°/33.3°
Telescope plate scale at slit	3.27 arcsec/mm
Plate scale reimaged on mosaic array	0.88 arcsec/pixel
Slit Dimensions (width adjustable)	1 mm x 16 mm
Spectral sampling interval (8-14 μ m)	0.2 to 0.1 micron
Point source spectral resolution (8-14 μ m)	0.2 to 0.1 micron



Accession For	
NTIS GRA&I	<input checked="" type="checkbox"/>
DTIC TAB	<input type="checkbox"/>
Unannounced	<input type="checkbox"/>
Justification	
By	
Distribution/	
Availability Codes	
Dist	Avail and/or Special
A-1	

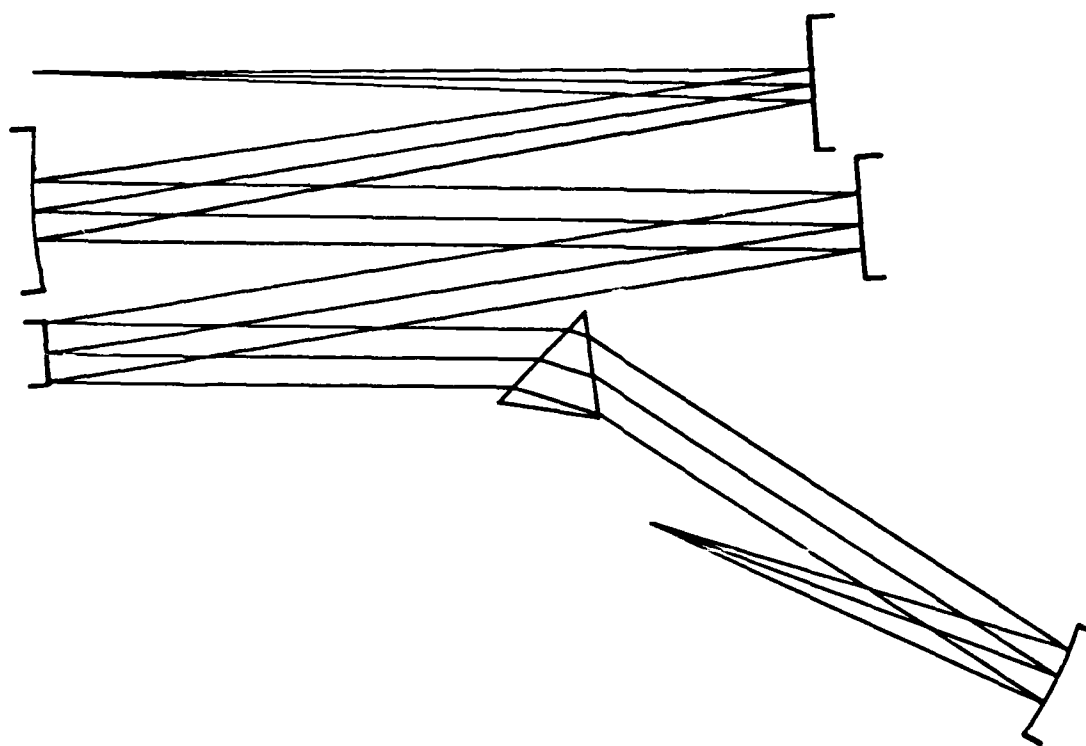


Fig. 1. Sodium Chloride prism spectrometer 80% full scale ray trace. Two additional folding mirrors are not shown in this equivalent "flat" layout. The slit (not shown) is at the telescope focus (upper left) whereas the mosaic array is at the camera focus (lower left). Trace is made for 11 micron rays.

The spectrometer design described above was built by Wentworth Institute of Technology (Boston, MA) and Sensor Systems Group (Waltham, MA). Because of the requirement that the collimator be midway between the slit and the Lyot stop and at a distance from each equal to its focal length, several flat mirror foldings of the beam are required. The 11 micron ray trace for an equivalent flat, as opposed to stacked system is shown in Figure 1, and a photograph of the "stacked" assembly is shown in Figure 2. The spectrometer is made of aluminum throughout, with all mirror substrates mounting surfaces stress relieved to preserve alignment as the system is cooled to liquid helium temperature.

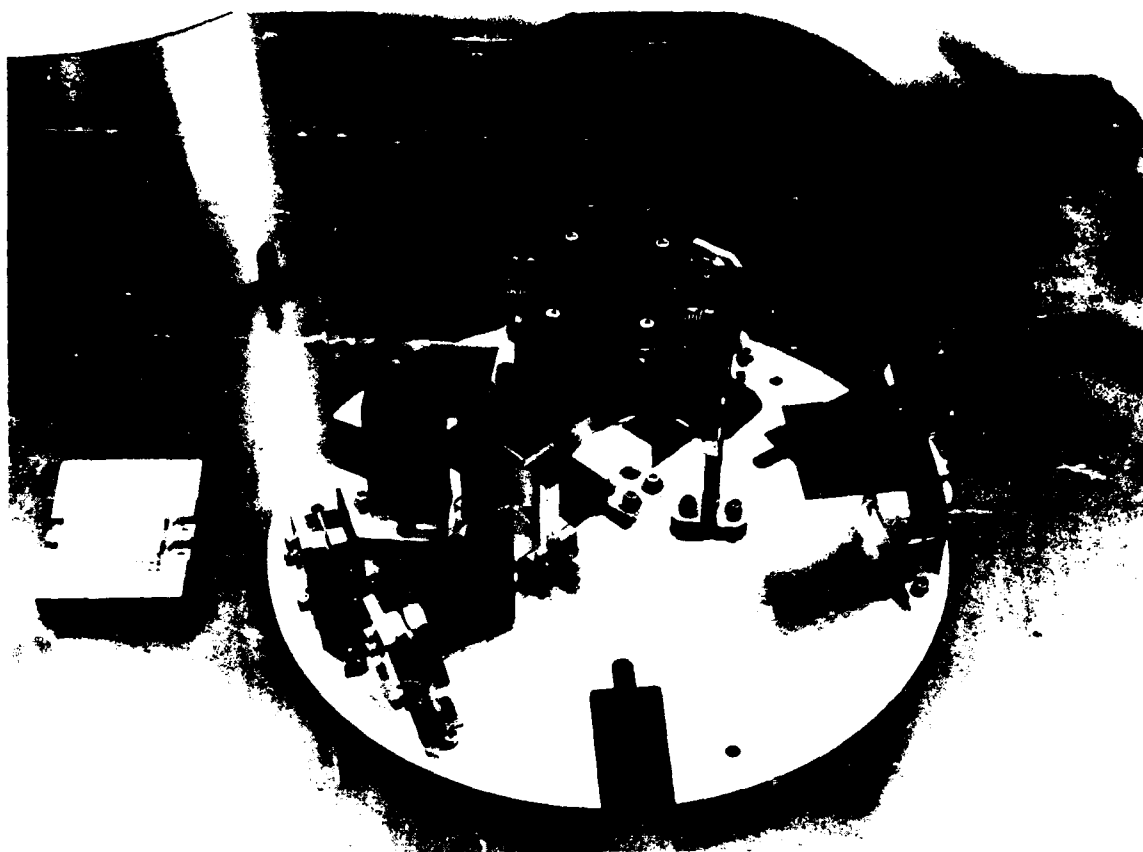


Fig. 2. Assembled slit spectrometer and optics baseplate. Easily seen in this view are the adjustable slits, collimator mirror (closest to ruler), and prism.

The overall transmission of the optics assembly at 11 microns derives from reflection coefficients for the 7 mirrors, (0.7, where $r = 0.95$ is assumed for a single Nickel-coated Aluminum surface), and the 11 micron transmission factors for the 1.5 mm thick Barium Fluoride dewar window (0.87) and for the coated Sodium Chloride prism (0.92), for an overall transmission of 55%.

The aberrations in the spectrometer result from the spherical rather than parabolic collimating and camera mirrors surfaces, the off-axis astigmatism, and coma. These blurs were all found smaller than the ten micron diffraction blur of the 2.3 meter telescope. Sagittal coma is also reduced in this Czerny-Turner design.

The alignment of the spectrometer assembly was performed at room temperature with a Helium-Neon laser (6328A). It was divided into the

internal spectrometer alignment and the relative spectrometer and mosaic array alignment. The two translational degrees of freedom for the latter are specified by requiring the slit-centered laser beam to fall on the spatial centerline of the array at the calculated distance from the spectral centerline to the HeNe spot (5.25mm). The single rotational degree of freedom aligns the spectral/spatial axes with the mosaic array edges. The optics assembly was rotated such that scanning the laser beam parallel to a slit edge resulted in scans parallel to the mosaic edges.

IV. LABORATORY PERFORMANCE ASSESSMENT

A number of fundamental issues were addressed during the initial stages of the IR mosaic spectrometer construction. Most fundamental among these related to the question of electronically scanning the array sufficiently rapidly to prevent saturation under groundbased background radiation conditions. A related question was that of the linearity of the array over these operating conditions - would doubling the integration time for a fixed amount of radiation falling on the detectors double the output signal? These questions were both addressed in a "test bed" dewar incorporating a resistor on thermally - insulated substrate and in the Field of View of the mosaic array, which would be cold (and have no infrared emission) until a current is applied. Initially, the system could not handle significant radiation levels from the heating resistor due to a relatively shallow slope (10 usec/volt) of reset time as a function of signal voltage - a decrease in source follower resistance from 100 k Ω to 10 k Ω along with an increase of the on-chip source follower gate voltage from 0.7 to 0.8 volts improved the reset time for a 1 volt signal level from 10 usec to 1 usec. (This conclusion has been confirmed and elucidated by Dr. M. Hewitt of SBRC). The array bias voltages are generally those used in the GSFC testing of a similar array under low background conditions [Lamb et al. 1986], with the exception just noted). The corresponding minimum integration time of 5.4 msec is the total number of pixels (3596) divided by the number of output lines (2) and multiplied by the pixel address window duration (3 usec) sufficiently long for equilibrium level attainment of clamping and sampling levels. This value of integration time is sufficiently short to permit the photon arrival rates expected on the 2.3 meter telescope for one arcsec pixels and for a 0.1 micron spectral bandpass.

Having shown the feasibility of operation of the mosaic array under the expected background radiation levels, it was next necessary to ascertain linearity of operation over these background levels. This was accomplished by selecting resistor current, allowing equilibrium conditions, and scanning the array first in its entirety and secondly only either the top or bottom one half of the array. Since the integration time for any given pixel is directly proportional to the number of pixels read per frame, the integration time for full scan array is exactly twice that for the one-half array scan. Repeating this for incremental changes

of resistor current probed the linearity over a range extending from the noise floor up to saturation of the analog to digital convertor. Plotting $S(\tau_{2.7})$ against $S(\tau_{5.4})$, where $\tau_{2.7}$ denotes the shorter (2.7 msec) integration time and $\tau_{5.4}$ the larger (5.4 msec) time, results in an acceptable correlation. The fit to the data of a straight line with non-zero intercept indicates that after subtraction of system offset, the system is linear (slope 2) to within 10%, an uncertainty compatible with the scatter in the data points.

V. PERFORMANCE ASSESSMENT AT THE TELESCOPE

Having characterized the performance of the IR Array Spectrometer in the laboratory for linearity and noise level, full operational capability was demonstrated at the University of Wyoming 92 inch telescope outside of Laramie, Wyoming.

On the night of 9 February 1987, the bright infrared source IRC + 10216 was measured by scanning the entire mosaic array, in contrast to earlier single pixel detections. The resulting data consist of several rows of 31 pixels each corresponding to the spatial extent, with each pixel in a given row corresponding to a wavelength value. Because the general spectral shape of IRC + 10216 may be approximated by a blackbody, (we ignore for the present purposes the variable SiC feature) it can be removed from each individual row. The resulting spectrum (Figure 3) embodies the transmission of the atmosphere as well as responsivity variations with both pixel number and with wavelength for a given pixel, and wavelength-dependent transmission factors for the Barium Fluoride dewar window and, less important, the Sodium Chloride prism. The "wavelength calibration", or association of wavelength value and row pixel number, can be crudely derived as a result. The derivation is based on solutions to the prism equation for a fixed (48°) angle of incidence and deviation angles corresponding to pixel spacings and the camera mirror focal length (0.075mm and 75mm, respectively). A baseline shift is effectuated by requiring a position match of the atmospheric ozone absorption. With the wavelength calibration program run according to these conditions, the Pixel 31 wavelength is 7.85 microns, the Pixel 1 wavelength is 14.25 microns, and the predicted HeNe laser ($\lambda 6328\text{\AA}$) distance is 5.3mm from the array center. Therefore, the optics alignment discussed in Section 3 for which the value of 3mm was used for the distance from HeNe point to array edge was on the mark. Also, negligible misalignment between room temperature and 4°K is indicated, a valuable confirmation of the thermal stress reduction design implemented by Sensor Systems Group. Remembering that instrumental factors involving pixel responsivities and window transmission functions affect the overall shape, the fine structures of the spectrum in Figure 3 compare favorably with those of the atmospheric transmission calculation (AFGL LOWTRAN) presented in Figure 4. The accuracy of the preliminary wavelength calibration is a fraction of the ozone feature width, or about 0.2 micron.

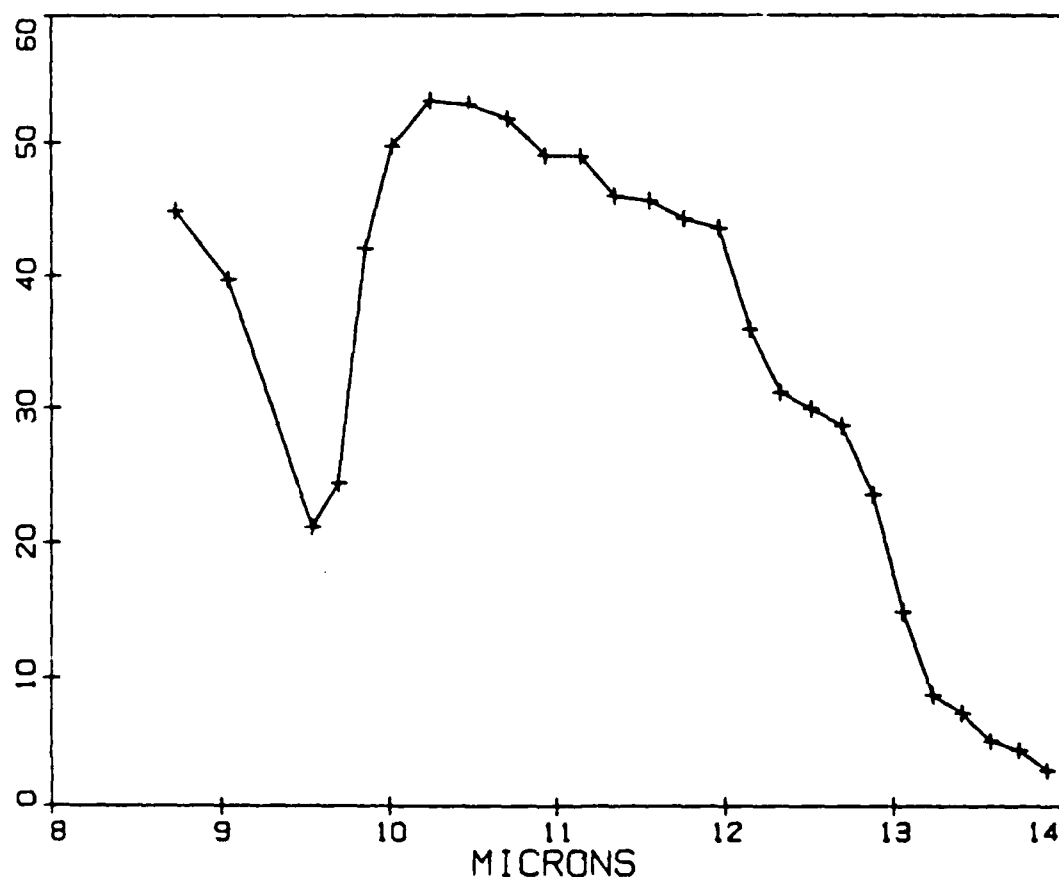


Fig. 3 Atmospheric transmission and instrumental response as determined by scans of IRC + 10216. The data correspond to the 31 pixels in a single column, with 4 edge pixels deleted. The observed star, IRC = +10216, has been approximately removed as discussed in the text. Compare with Figure 4.

Regarding the spatial characterization of the array spectrometer, the most important attribute is the image blur Full Width Half Maximum (FWHM). The cuts along the spatial direction at the wavelengths of 9, 11.8 and 12.5 microns are shown as a function of row number (1 to 58, total) in Figure 5. (The baseline is presumably due to the cumulative effects of the difference in telescope background between the two chop positions over the many coadded frames of data. If this is indeed the case, future data acquisition methods involving "beam switching" of the telescope will cancel the baseline). The FWHM values for the three spatial scans is 3.1 pixels, which for a plate scale 0.88 arcsec/pixel

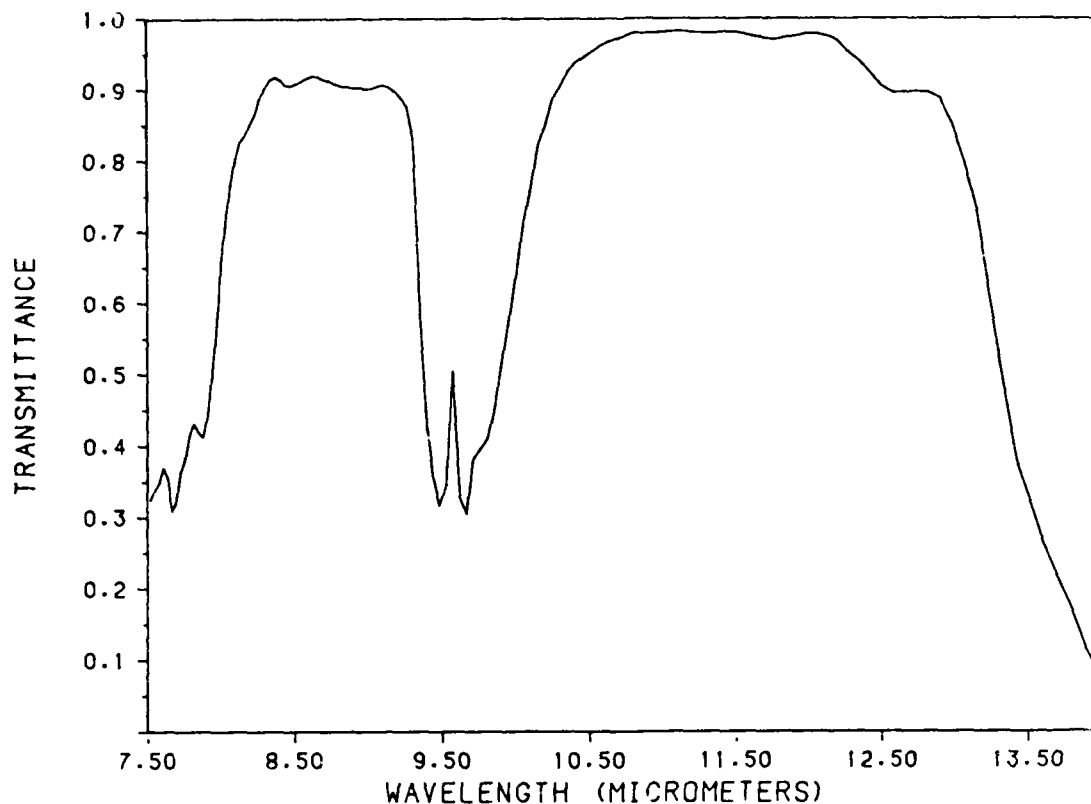
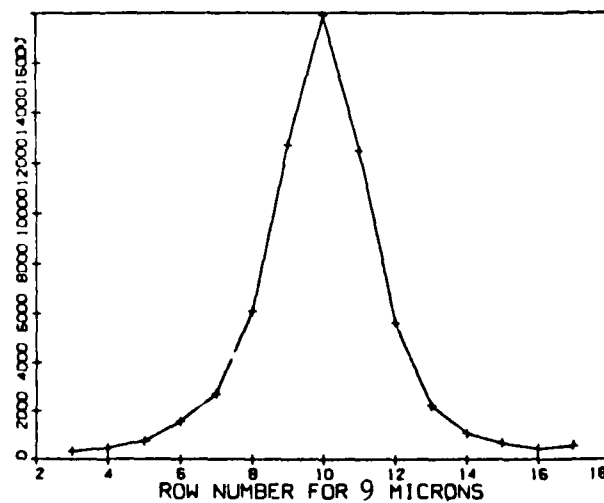
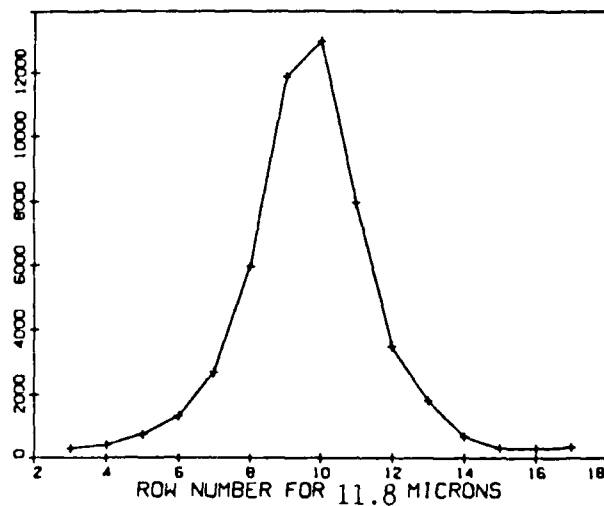
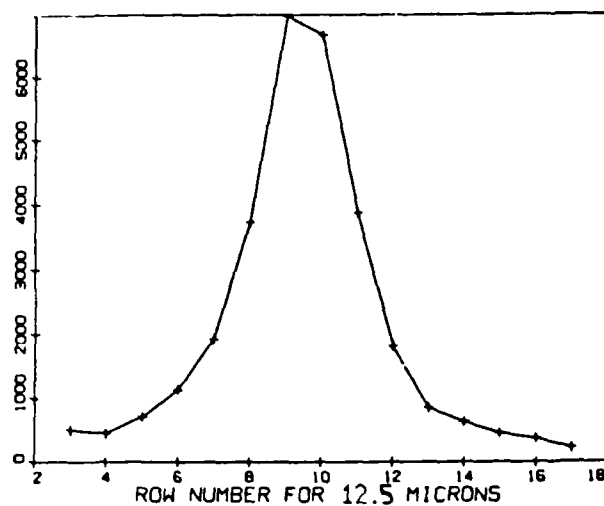


Fig. 4. Predicted LOWTRAN transmission for a high and dry site. The atmosphere is midlatitude winter, the height is 2 Km, and the zenith angle is zero. Line of sight water vapor is less than 1mm, typical of good conditions on Jelm Mountain. Compare with Figure 3.

corresponds to approximately 2.7 arcsecs. This is to be compared with the combined telescope and spectrometer diffraction blurs which are of equivalent linear size at the spectrometer focus. As IRC + 10216 is extended at ten microns on the scale of fractional arcsecs, it cannot be determined if the FWHM values result from a non-optimal focus or represent true source structure. This awaits quantification during subsequent observing runs.

The remaining performance assessment to be gleaned from these data is the ultimate sensitivity attainable, which is currently limited by the number of output bits for A to D convertors capable of 500 MHz or higher conversion rates. From repeated data collections, it is estimated that the signal to noise in the 10.0 micron channel after one frame

Fig. 5. Spatial scans through IRC + 10216 at wave-lengths of 12.5(top), 11.8(middle), and 9 (bottom) microns. The row spacing is 0.9 arcsec.



(10.8 msec integration time) of IRC + 10216 is 52, and after coadding 80 frames (0.84 sec integration time) is 300. Assuming square root time improvement in signal to noise after approximately 3000 sec the 10 Jansky threshold of the IRAS Low Resolution Spectrometer could be attained with the present 12 bit A to D convertor.

Acknowledgements. We are pleased to acknowledge the valuable contributions of Dr. S. Little in the design of the optics layout, of T. Campbell, P. Hurly, and D. Nardello for construction of the system electronics and optics, and to D. Wang and R. Benoit for optical finish and alignment. The contributions of staff and graduate students at Wyoming Infrared Observatory were also valuable to the success of the project. Dr. William Ewing is acknowledged for valuable conversations on the essentials of the electronics design.

Postscript. Since the Hilo Detector Array Workshop, 5 more objects bright at ten microns have been measured with the Array Spectrometer with short (1 second) exposures.

References

- Lamb, G.M., Shu, P.S., Lokerson, D.C., Gezari, D.Y., Bowser, J., 1986, in Proceedings of the Second Infrared Detector Technology Workshop, ed. C.R. McCreight (NASA Tech. Memo, 88213), p. 25-1.
- White, M.H., Lampe, D.R., Blaha, F.C. and Mack, I.A. 1974, IEEE J. Solid State Electronics, 9, p. 1.

END

DATE

FILMED

DTIC

10-88